



Mutations in *KIF7* link Joubert syndrome with Sonic Hedgehog signaling and microtubule dynamics

Claudia Dafinger,^{1,2} Max Christoph Liebau,^{2,3} Solaf Mohamed Elsayed,^{4,5} Yorck Hellenbroich,⁶ Eugen Boltshauser,⁷ Georg Christoph Korenke,⁸ Francesca Fabretti,² Andreas Robert Janecke,⁹ Inga Ebermann,¹ Gudrun Nürnberg,^{10,11} Peter Nürnberg,^{10,11} Hanswalter Zentgraf,¹² Friederike Koerber,¹³ Klaus Addicks,¹⁴ Ezzat Elsobky,^{4,5} Thomas Benzing,^{2,11} Bernhard Schermer,^{2,11} and Hanno Jörn Bolz^{1,15}

¹Institute of Human Genetics and ²Renal Division, Department of Medicine and Centre for Molecular Medicine, and ³Department of Pediatrics, University of Cologne, Cologne, Germany. ⁴Medical Genetics Center, Cairo, Egypt. ⁵Children's Hospital, Ain Shams University, Cairo, Egypt. ⁶Institute of Human Genetics, University Hospital of Schleswig-Holstein, Campus Lübeck, Germany. ⁷Department of Paediatric Neurology, University Children's Hospital of Zurich, Zurich, Switzerland. ⁸Klinikum Oldenburg, Zentrum für Kinder- und Jugendmedizin, Elisabeth Kinderkrankenhaus, Neuropädiatrie, Oldenburg, Germany. ⁹Department of Pediatrics II, Innsbruck Medical University, Innsbruck, Austria. ¹⁰Cologne Center for Genomics and Centre for Molecular Medicine, University of Cologne, Cologne, Germany. ¹¹Cologne Excellence Cluster on Cellular Stress Responses in Aging-Associated Diseases, University of Cologne, Cologne, Germany. ¹²Department of Tumor Virology, German Cancer Research Center, Heidelberg, Germany. ¹³Department of Radiology and ¹⁴Department of Anatomy, University of Cologne, Cologne, Germany. ¹⁵Bioscientia Center for Human Genetics, Ingelheim, Germany.

Joubert syndrome (JBTS) is characterized by a specific brain malformation with various additional pathologies. It results from mutations in any one of at least 10 different genes, including *NPHP1*, which encodes nephrocystin-1. JBTS has been linked to dysfunction of primary cilia, since the gene products known to be associated with the disorder localize to this evolutionarily ancient organelle. Here we report the identification of a disease locus, *JBTS12*, with mutations in the *KIF7* gene, an ortholog of the *Drosophila* kinesin *Costal2*, in a consanguineous JBTS family and subsequently in other JBTS patients. Interestingly, *KIF7* is a known regulator of Hedgehog signaling and a putative ciliary motor protein. We found that *KIF7* co-precipitated with nephrocystin-1. Further, knockdown of *KIF7* expression in cell lines caused defects in cilia formation and induced abnormal centrosomal duplication and fragmentation of the Golgi network. These cellular phenotypes likely resulted from abnormal tubulin acetylation and microtubular dynamics. Thus, we suggest that modified microtubule stability and growth direction caused by loss of *KIF7* function may be an underlying disease mechanism contributing to JBTS.

Introduction

Joubert syndrome (JBTS) is a rare, mostly autosomal recessively inherited developmental disorder characterized by cerebellar hypoplasia, ataxia, psychomotor delay, and an altered respiratory pattern in the neonatal period. Retinal degeneration, renal cysts, liver fibrosis, and skeletal involvement can be present. The hallmark of JBTS is a midbrain-hindbrain malformation, named “molar tooth sign” (MTS) because of its appearance on axial magnetic resonance imaging. The 10 genes implicated in JBTS, *CEP290*, *TMEM67*/*MKS3*, *RPGRIP1L*, *ARL13B*, *AH11*, *NPHP1*, *CC2D2A*, *INPP5E*, *TMEM21*, and *OFD1*, all play a role in the formation or function of sensory cilia (1). Primary cilia are essential for vertebrate development, and mutations affecting this organelle underlie a large group of human malformation syndromes, the ciliopathies (2). Cilia are antenna-like protrusions on the cell surface, covered by the plasma membrane and containing a ring of 9 microtubule doublets. Studies in mutants with defective ciliogenesis revealed that cilia are essential for vertebrate Hedgehog (Hh) signaling, a pathway that is crucial for embryonic patterning, organogenesis, and tumor formation (3).

Most JBTS genes have been identified through linkage analysis in consanguineous families. Using such an approach, we have mapped a novel JBTS locus, *JBTS12*, to chromosome 15q25.3–q26.3 in an Egyptian family. One gene in that locus, *KIF7* (GenBank NM_198525), represented a prime candidate for the novel JBTS subtype because of its assumed dual roles as a Sonic Hedgehog (Shh) pathway component and a ciliary motor protein (3). Here, we identify *KIF7* as a JBTS-causing gene, and our functional studies suggest that *KIF7* is closely linked to the biology of cilia, centrosomes, and the Golgi network by regulating the stability and dynamics of microtubules.

Results and Discussion

Mapping of a locus for Joubert syndrome, JBTS12, to chromosome 15q. In a consanguineous Egyptian family with 2 JBTS individuals, designated E1 and E2 (Figure 1, A and D), genome-wide linkage analysis revealed a 15.3-Mb region with homozygosity by descent on chromosome 15q25.3–q26.3 (between SNPs rs717552 and rs352744). This locus for Joubert syndrome has been registered as *JBTS12* (HGNC accession code for *KIF7* [alias *JBTS12*]: 30497) and contained approximately 85 genes, and candidates were prioritized by expression pattern and/or structure. No mutations were found in *TTC23*, *NTRK3*, and *RLBP1*. We then focused on *KIF7*, an essential regulator of Shh signaling localized in cilia. Notably, the JBTS proteins *ARL13B* and *RPGRIP1L* are implicated in Shh signaling (4, 5).

Authorship note: Claudia Dafinger, Max Christoph Liebau, and Solaf Mohamed Elsayed contributed equally to this work.

Conflict of interest: The authors have declared that no conflict of interest exists.

Citation for this article: *J Clin Invest.* 2011;121(7):2662–2667. doi:10.1172/JCI43639.

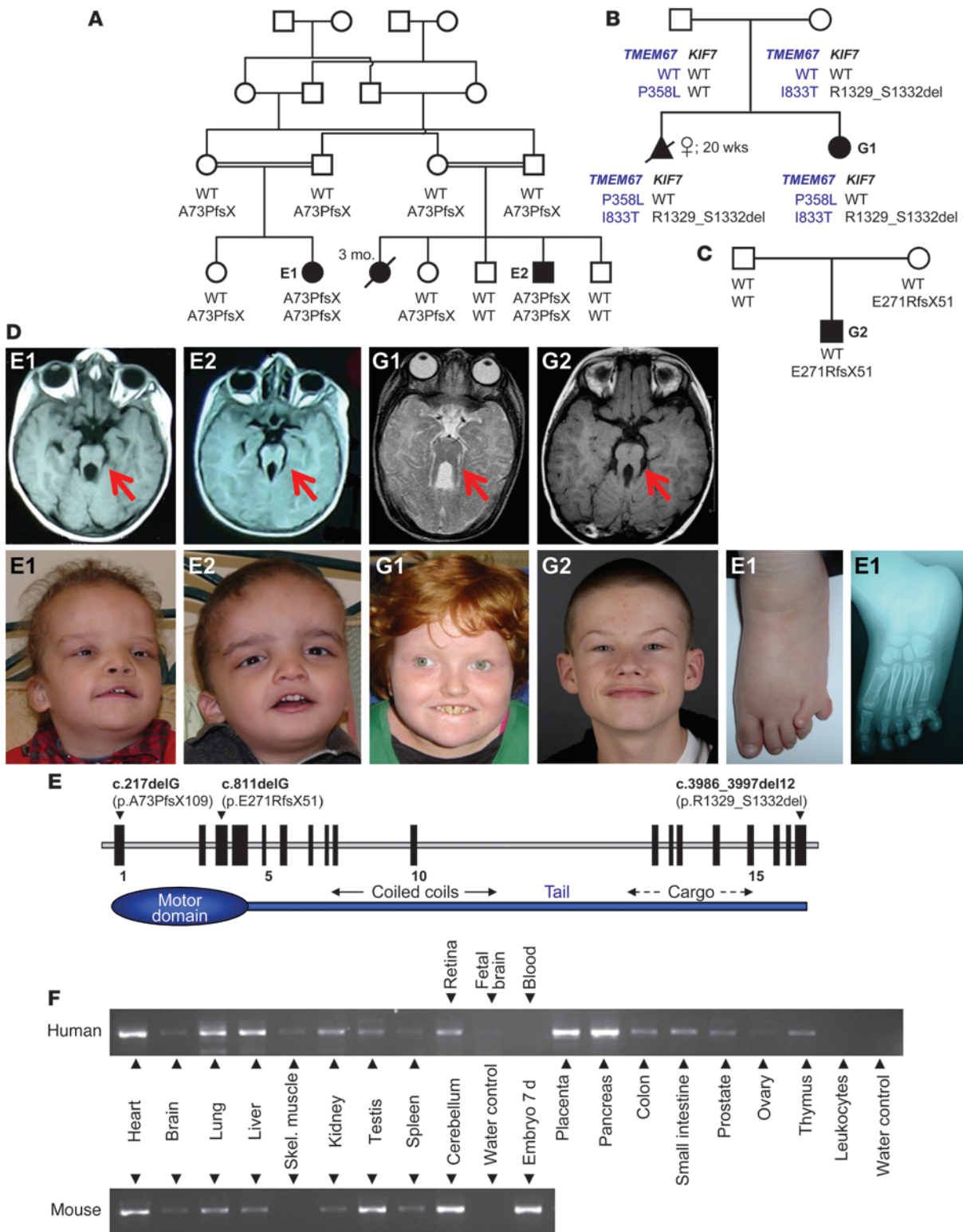


Figure 1

KIF7 mutations cause Joubert syndrome and define a novel disease locus, *JBTS12*. For clarity, the one-letter code was applied for mutation designation. **(A–C)** Pedigrees of JBTS families with *KIF7* mutations. **(A)** Egyptian index family. Linkage analysis in this family identified the 15q locus harboring *KIF7*. **(B)** G1 family. Abortion was induced in the first pregnancy because of an encephalocele. **(C)** G2 family. **(D)** Top: Axial brain MRIs showing molar tooth sign (red arrow) from the affected members of each family. Bottom: Dysmorphic features characteristic of JBTS (pronounced in E1 and E2, with hexadactyly in E1 and hypertelorism in G1). No dysmorphism in G2. **(E)** *KIF7* gene structure (drawn to scale), mutations, and protein illustration. **(F)** Expression profile of human and mouse *KIF7* (RT-PCR).



Table 1
Molecular and clinical findings in JBTS patients with *KIF7* mutations

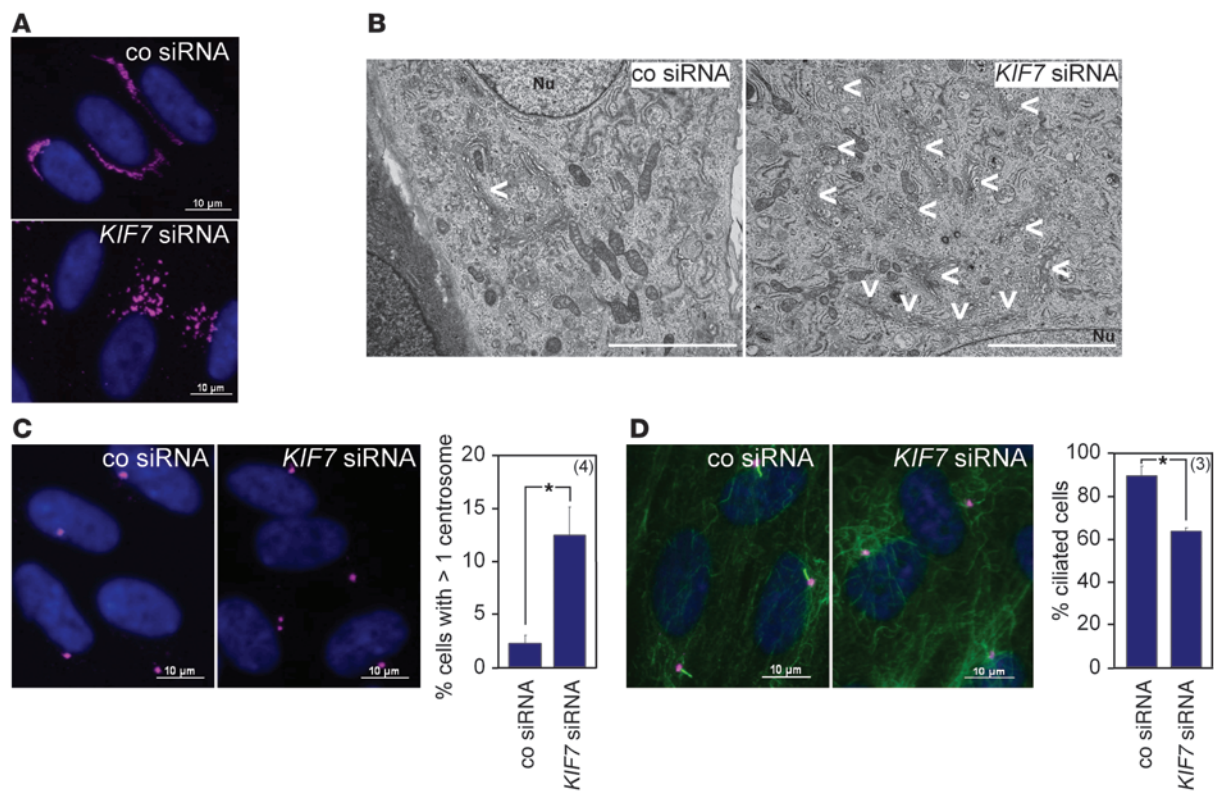
Patient	Age (yr)	<i>KIF7</i> mutations	Controls without mutation	Other JBTS gene mutations ^a	MR	Ataxia	cMRI	Encephalocele	Polydactyly	Facial dysmorphism	Renal disease	Liver disease	Retina
E1	6	c.217delG (exon 1)	104	-	++	++	MTS, ACC	-	LH, RH, LF	HT, TM, DPF, DSE, PF	-	-	-
E2	4	c.217delG	104	-	++	-	MTS	-	-	HT, TM, DPF, DSE, PF	-	-	-
G1	9	c.3986_3997del (exon 18)	332	p.P358L (<i>TMEM67</i>) p.I833T (<i>TMEM67</i>)	+	+	MTS	-	-	HT, DSE	-	ELE	COL (LE)
G2	17	c.811delG (exon 3)	114	-	+	-	MTS	-	-	-	-	-	-

^aAmong the genes implicated in JBTS: *CEP290*, *TMEM67*, *RPGRIP1L*, *ARL13B*, *AH11*, *NPHP1*, *CC2D2A*, *INPP5E*, *TMEM216*. Severity of MR and ataxia is indicated as follows: +, mild; moderate; ++, severe. ACC, agenesis of the corpus callosum; COL, coloboma; DPF, downslanting palpebral fissures; DSE, deep-set ears; ELE, elevated liver enzymes; HT, hypertelorism; LE, left eye; LF, left foot; LH, left hand; MR, mental retardation; PF, prominent forehead; RH, right hand; TM, triangular mouth.

Loss of *Kif7* function in mice results in polydactyly, exencephaly, skeletal defects, and early lethality (6–8), symptoms reminiscent of both Hedgehog pathway mutants and JBTS mouse models, e.g., *Inpp5e*^{-/-} mice (9). RT-PCR revealed widespread expression of *KIF7* (Figure 1F) and, consistent with RNA in situ hybridization data (available at Allen Mouse Brain Atlas, <http://mouse.brain-map.org>), strong expression in the cerebellum.

Mutations of KIF7 cause JBTS. We identified a homozygous 1-bp deletion in exon 1 of *KIF7* (c.217delG) that segregates with the phenotype and results in either a heavily truncated protein (p.A73PfsX109) or nonsense-mediated decay. We extended the DNA analysis to 63 additional JBTS patients. A German girl (G1) carried a heterozygous 12-bp deletion in the last *KIF7* exon (c.3986_3997del12; Figure 1, B and D), predicting a likely deleterious in-frame loss of 4 residues in the putative *KIF7* cargo domain (Figure 1E). A male German patient (G2) carried a heterozygous truncating deletion in *KIF7* exon 3 (c.811delG; Figure 1C and Supplemental Figure 1; supplemental material available online with this article; doi:10.1172/JCI43639DS1). As no further *KIF7* mutations were detected by direct sequencing in patients G1 and G2, we performed array comparative genomic hybridization (CGH) on a NimbleGen array with probes densely covering the *KIF7* locus, as well as genome-wide CGH (Affymetrix 6.0 SNP array). Neither patient showed structural alterations adjacent to or within *KIF7* (Supplemental Figure 2), or the relatively frequent *NPHP1* deletion (10). Sequencing of all known autosomal JBTS genes revealed 2 *TMEM67* mutations, p.P358L and p.I833T, in patient G1, but no mutations in G2. The most severe phenotype was observed in patients E1 and E2 with biallelic loss of *KIF7*. In G1, mental retardation and facial dysmorphism were less pronounced. The 2 hypomorphic *TMEM67* mutations have frequently been found in patients with COACH (JBTS with coloboma and hepatic fibrosis), but never in combination (11, 12). Disease in G1 may result from the mutational load, with 3 mutant alleles in 2 JBTS genes, similar to what has been shown for patients with a distinct ciliopathy, Bardet-Biedl syndrome (13). In G2, either a mutation in a functionally related gene not yet implicated in JBTS or a second *KIF7* mutation that escaped detection due to its localization (e.g., deep intronic or in a regulatory region outside the coding sequence) is likely. The phenotype of G2 is relatively mild, with moderate developmental delay and no dysmorphic signs (Table 1).

Defects of cilia formation and centrosome duplication and fragmentation of the Golgi network in KIF7-deficient cells. To address the pathophysiologic mechanisms of *KIF7* deficiency, we transfected siRNA directed against the 3'-untranslated region (3'-UTR) of *KIF7* mRNA in polarized retinal epithelial cells (Supplemental Figure 3) and assayed for the cellular phenotype. *KIF7*-deficient cells displayed a dispersed staining pattern of the Golgi apparatus (Figure 2A, Supplemental Figures 4 and 6), a phenotype that had been previously observed in cells deficient for the kinesin-2 subunits KAP3 and KIF3A (14). Transfection of the *KIF7* coding sequence into knockdown cells was able to rescue this phenotype, whereas expression of a protein lacking the predicted motor domain (*KIF7*₅₁₃₋₁₃₄₃) did not (Supplemental Figure 5), indicating that the knockdown phenotype was the result of defective *KIF7* motor activity. Strikingly, expression of the latter truncation also induced a dispersed Golgi staining pattern similar to the one observed in knockdown cells, suggesting a crucial role of the predicted *KIF7* motor domain for maintaining Golgi structure (Supplemental Figure 5). Electron microscopy confirmed disruption of regular Golgi patterning in

**Figure 2**

KIF7 is required for Golgi, centrosomal, and ciliary integrity. siRNA knockdown results in dispersal of the Golgi apparatus as seen in (A) immunofluorescence stainings for golgin-97 and (B) electron microscopy (arrows indicate Golgi fields; co, control; Nu, nucleus). While Golgi stacks in control cells are mainly found in the perinuclear region, Golgi-derived vesicles and enlarged Golgi fields are widely distributed between the nucleus and the apical membrane in knockdown cells. (C) Moreover, KIF7 knockdown cells show abnormal centrosomal duplication and (D) a reduced number of cilia. Scale bars: 10 μ m (A, C, and D); 5 μ m (B). * $P < 0.05$ in an unpaired Student's t test.

KIF7 siRNA-treated cells (Figure 2B); however, a marked general Golgi transport defect could not be demonstrated, as labeled VSV-G protein did not show apparent deficiencies in membrane delivery (not shown). Golgi dispersal was also observed with siRNAs directed against the protein-coding sequence of KIF7 (Supplemental Figures 7 and 8). In addition to the dramatic changes in Golgi structure, we observed more subtle defects such as abnormal centrosome duplications and a reduced number of ciliated cells (Figure 2, C and D), reminiscent of previously reported findings in other JBTS proteins (15).

KIF7 interacts with the JBTS4 protein NPHP1. Since several human ciliopathy proteins function in multiprotein complexes to regulate cilia formation, microtubule dynamics, or Golgi structure, we tested whether KIF7 interacted with known JBTS proteins. Intriguingly, KIF7 specifically co-precipitated with nephrocystin-1 (NPHP1) and vice versa (Supplemental Figure 9). Mapping of the interaction revealed that amino acids 513–775 of KIF7 were sufficient for co-precipitation of NPHP1 (Supplemental Figure 9). Immunofluorescence stainings of NPHP1 in KIF7-knockdown cells showed a redistribution of NPHP1 as a result of the Golgi phenotype (Supplemental Figure 10). The JBTS1 protein INPP5E also localizes to the Golgi apparatus (16). However, in contrast to INPP5E, KIF7 did not influence PDGF-induced phosphorylation of AKT (Supplemental Figure 11), pointing to potentially divergent molecular mechanisms of disease. Taken together, these data

suggest that KIF7 either acts through directly regulating Golgi morphology and function or that the Golgi phenotype results from a cellular defect of membrane fusion, vesicle targeting, or cytoskeletal regulation.

KIF7 affects microtubular dynamics. We have previously shown that ciliopathy disease proteins may associate with or act through microtubule regulatory proteins (17). Since defects in microtubular dynamics can result in Golgi disruption (18), defects in ciliogenesis (19), and altered cell morphology, we reasoned that the KIF7 phenotype may be the result of altered microtubular dynamics. Interestingly, expression of KIF7₅₁₃₋₁₃₄₃ as well as knockdown of KIF7 led to a marked stabilization of acetylated microtubules on ice (Figure 3A and Supplemental Figure 12A). The histone deacetylase HDAC6 has recently been linked to the regulation of cytoplasmic microtubule acetylation by the Bardet-Biedl syndrome protein BBIP10 (19). Strikingly, HDAC6 specifically co-precipitated with KIF7 (Supplemental Figure 12B), and expression of KIF7₅₁₃₋₁₃₄₃ led to an increase in acetylated tubulin in HEK293T cells (Supplemental Figure 12C). These data indicated that KIF7 is involved in the regulation of microtubule acetylation and stabilization. Because stabilization of microtubule and lack of the microtubule dynamics have been shown to induce Golgi dispersal (20), microtubule overstability likely explains the cellular KIF7 phenotypes observed in our study. Moreover, we demonstrate maloriented microtubular growth after KIF7 knockdown in microtubular re-polymerization

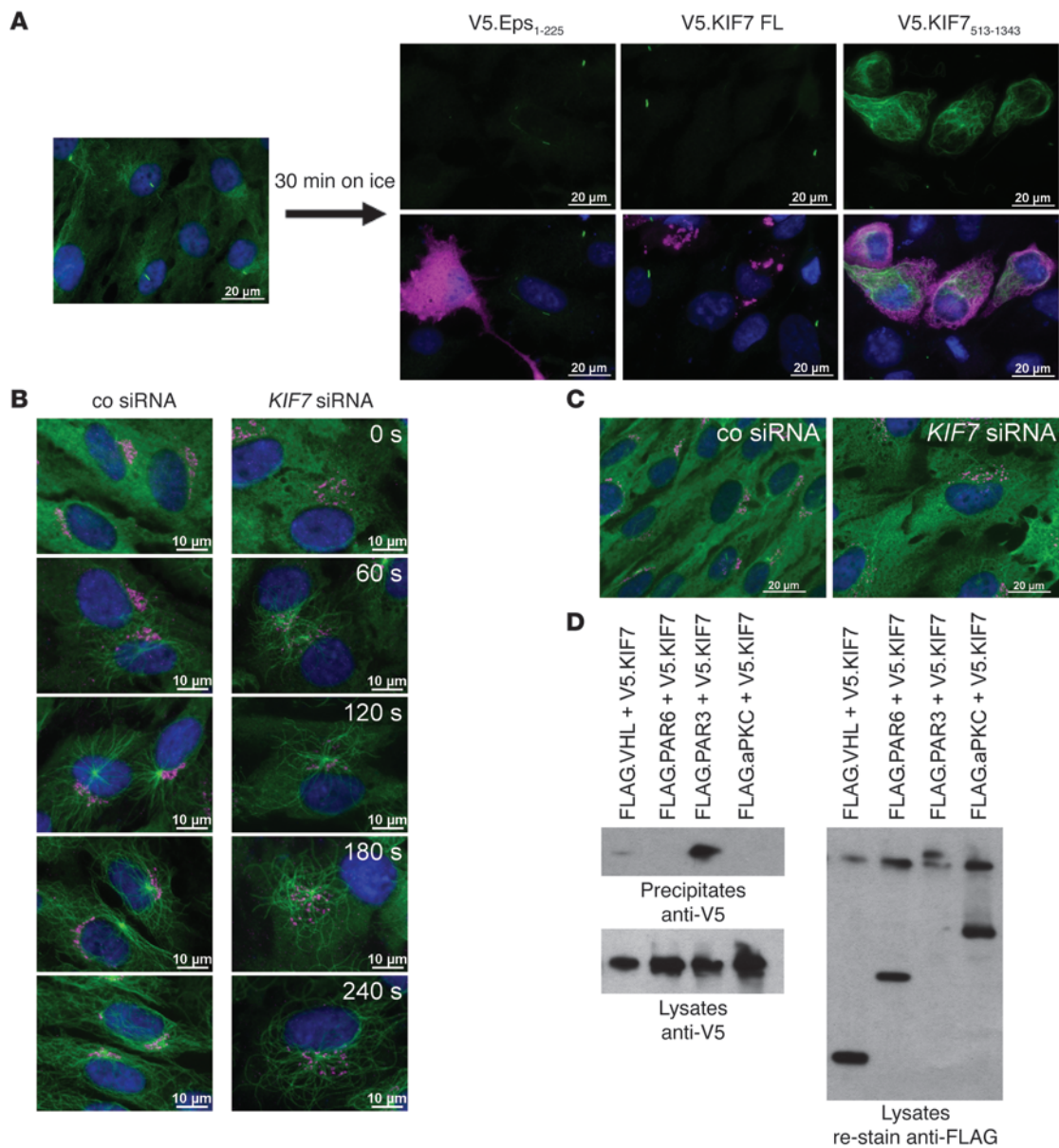


Figure 3 KIF7 dysfunction affects microtubular stability and dynamics. **(A)** In hTERT-RPE1 cells expressing KIF7₅₁₃₋₁₃₄₃, acetylated microtubules are resistant to de-polymerization on ice. **(B)** Re-polymerization of microtubules in *KIF7* knockdown cells is less coordinated. **(C)** *KIF7* knockdown cells display changes in the cell shape. **(D)** KIF7 interacts with the polarity protein PAR3. PAR3 is specifically able to precipitate KIF7. Scale bars: 20 μm (**A** and **C**); 10 μm (**B**).

assays (Figure 3B), and we noticed differences in the shape of cells treated with *KIF7* siRNA (Figure 3C). When looking for potential KIF7-interacting regulators of directed microtubular growth, we found PAR3 to be associated with KIF7 (Figure 3D).

KIF7 has recently been shown to be a key regulator of vertebrate Shh signaling that localizes to the ciliary base and translocates to the ciliary tip upon pathway activation by ligand binding (8). Our findings link KIF7 with Golgi morphology, centrosomal duplication, ciliogenesis, and Hedgehog signaling. We propose modified microtubule stability and growth direction caused by loss of KIF7 function as the underlying disease mechanism impacting all these structures and processes, ultimately resulting in JBTS.

Besides, *KIF7* represents a prime candidate for mono- and oligogenic forms of related ciliopathies, namely Meckel-Gruber, Senior Loken, and Bardet-Biedl syndromes, Leber congenital amaurosis, and nephronophthisis.

Methods

Patients. The study was approved by the review boards of the Ethics Committees of the University Hospitals of Cologne, Schleswig-Holstein, and Zurich. Biological samples were donated by the patients after their parents provided written informed consent in accordance with the Declaration of Helsinki. The patients' parents gave written consent for displaying the photo images.



Genetic linkage analysis. See Supplemental Methods for details.

Mutation analyses. See Supplemental Methods for details.

Exclusion of large deletions and duplications involving KIF7 and NPHP1 in patients G1 and G2. The Affymetrix genome-wide Human SNP Array 6.0 utilizing more than 906,600 SNPs and more than 946,000 copy number probes was used for genome-wide detection of copy number variations. Quantitative data analyses were performed with GTC 3.0.1 (Affymetrix Genotyping Console) using HapMap270 (Affymetrix) as reference file. In addition, to detect and fine map potential deletions and/or duplications within *KIF7*, we performed oligonucleotide microarray CGH analysis. This analysis was carried out with a custom-designed high-resolution 385K array (Roche NimbleGen) with oligonucleotide probes (50mers to 75mers, spacing of approximately 20 bp).

Expression analysis. See Supplemental Methods for details.

Plasmids. The full-length coding sequence of *KIF7* was cloned by standard techniques using I.M.A.G.E. cDNA clones (BC042063, BC112271) and gene synthesis for bp c.1,188–1,553 (GenScript). The *HDAC6* coding sequence was PCR amplified from a human fetal brain library (Stratagene). The *NPHP1*, *gfp*, *Par3*, *Par6*, and *aPKC* plasmids have previously been described (17).

Antibodies, cell culture, and transfections. See Supplemental Methods for details.

RNAi experiments. *KIF7* and control siRNAs were purchased from Biomers or Ambion (Life Technologies) and had the following sequences: 5'-UUGUUGAUCCAGUGAGGGUATT-3' and 5'-UACCCUCACUG-GGAUCAACAATT-3' (siRNA#1, 3'-UTR), 5'-GCAAGUAUUUGA-CAAGGUTT-3' and 5'-ACCUUGUCAAAUACUUGCAG-3' (siRNA#2, coding sequence), and 5'-GUGACACGUUCGGAGAATTAC-3' and 5'-AATTCTCCGAACGUGUCACGU-3' (control siRNA).

Quantitative PCR. See Supplemental Methods for details.

Immunoprecipitation. Immunoprecipitations were performed as previously described (17). Experiments were repeated at least 3 times with identical results.

Immunofluorescence staining of hTERT-RPE1 cells. hTERT-RPE1 cells were seeded on glass slides, immunostained by standard techniques, and subjected to immunofluorescence microscopy (Axiovert 200 with ApoTome System, Zeiss).

De- and re-polymerization of microtubules. For de-polymerization, hTERT-RPE1 cells were incubated on ice for 30 minutes. Re-polymerization of microtubules was initialized by addition of prewarmed medium and stopped by fixation at the indicated time points.

Quantification of centrosomal duplication and cilia numbers. See Supplemental Methods for details.

Dual luciferase assay and electron microscopy. See Supplemental Methods for details.

Statistics. Data are expressed as mean \pm SEM of *n* experiments. Statistical evaluation was performed by using 2-tailed Student's *t* test. *P* values less than 0.05 were considered significant.

URLs. To predict the putative functional impact of the in-frame deletion in patient G1, we used MutationTaster, <http://neurocore.charite.de/MutationTaster/>. ScanProsite (<http://www.expasy.ch/tools/scanprosite>) was used for prediction of *KIF7* protein domains. Description of *KIF7* RNA in situ data relate to the corresponding entry in Allen Brain Atlas, <http://mouse.brain-map.org>.

Acknowledgments

We are indebted to the families who participated in this study. We thank Michaela Thoenes and Stefanie Keller for technical assistance. This work was supported by the Deutsche Forschungsgemeinschaft (BO2954/1-2 to H.J. Bolz; BE2212, SFB 832 to T. Benzing; SCHE1562, SFB 832 to B. Schermer), the Pro Retina Foundation Germany, Köln Fortune, and the Gertrud Kusen-Stiftung to H.J. Bolz.

Received for publication May 7, 2010, and accepted in revised form April 20, 2011.

Address correspondence to: Hanno J. Bolz, Bioscientia Center for Human Genetics, Konrad-Adenauer-Str. 17, 55218 Ingelheim, Germany. Phone: 496132.781.206; Fax: 496132.781.298; E-mail: hanno.bolz@uk-koeln.de. Or to: Bernhard Schermer, Renal Division, Department of Medicine, University of Cologne, Kerpener Str. 62, 50937 Cologne, Germany. Phone: 49.221.478.89030; Fax: 49.221.478.89041; E-mail: bernhard.schermer@uk-koeln.de.

1. Brancati F, Dallapiccola B, Valente EM. Joubert syndrome and related disorders. *Orphanet J Rare Dis.* 2010;5:20.
2. Gerdes JM, Davis EE, Katsanis N. The vertebrate primary cilium in development, homeostasis, and disease. *Cell.* 2009;137(1):32–45.
3. Goetz SC, Anderson KV. The primary cilium: a signalling centre during vertebrate development. *Nat Rev Genet.* 2010;11(5):331–344.
4. Cantagrel V, et al. Mutations in the cilia gene *ARL13B* lead to the classical form of Joubert syndrome. *Am J Hum Genet.* 2008;83(2):170–179.
5. Vierkotten J, Dildrop R, Peters T, Wang B, Ruther U. Ftm is a novel basal body protein of cilia involved in Shh signalling. *Development.* 2007;134(14):2569–2577.
6. Cheung HO, et al. The kinesin protein *Kif7* is a critical regulator of Gli transcription factors in mammalian hedgehog signaling. *Sci Signal.* 2009;2(76):ra29.
7. Endoh-Yamagami S, et al. The mammalian *Cos2* homolog *Kif7* plays an essential role in modulating Hh signal transduction during development. *Curr Biol.* 2009;19(15):1320–1326.
8. Liem KF Jr, He M, Ocbina PJ, Anderson KV. Mouse *Kif7/Costal2* is a cilia-associated protein that regulates Sonic hedgehog signaling. *Proc Natl Acad Sci USA.* 2009;106(32):13377–13382.
9. Jacoby M, et al. INPP5E mutations cause primary cilium signaling defects, ciliary instability and ciliopathies in human and mouse. *Nat Genet.* 2009;41(9):1027–1031.
10. Parisi MA. Clinical and molecular features of Joubert syndrome and related disorders. *Am J Med Genet C Semin Med Genet.* 2009;151C(4):326–340.
11. Doherty D, et al. Mutations in 3 genes (*MKS3*, *CC2D2A* and *RPGRIP1L*) cause COACH syndrome (Joubert syndrome with congenital hepatic fibrosis). *J Med Genet.* 2010;47(1):8–21.
12. Otto EA, et al. Hypomorphic mutations in meckelin (*MKS3/TMEM67*) cause nephronophthisis with liver fibrosis (*NPHP11*). *J Med Genet.* 2009;46(10):663–670.
13. Leitch CC, et al. Hypomorphic mutations in syndromic encephalocele genes are associated with Bardet-Biedl syndrome. *Nat Genet.* 2008;40(4):443–448.
14. Stauber T, Simpson JC, Pepperkok R, Vernos I. A role for kinesin-2 in COPI-dependent recycling between the ER and the Golgi complex. *Curr Biol.* 2006;16(22):2245–2251.
15. Valente EM, et al. Mutations in *TMEM216* perturb ciliogenesis and cause Joubert, Meckel and related syndromes. *Nat Genet.* 2010;42(7):619–625.
16. Kong AM, et al. Cloning and characterization of a 72-kDa inositol-polyphosphate 5-phosphatase localized to the Golgi network. *J Biol Chem.* 2000;275(31):24052–24064.
17. Schermer B, et al. The von Hippel-Lindau tumor suppressor protein controls ciliogenesis by orienting microtubule growth. *J Cell Biol.* 2006;175(4):547–554.
18. Cole NB, Sciaky N, Marotta A, Song J, Lippincott-Schwartz J. Golgi dispersal during microtubule disruption: regeneration of Golgi stacks at peripheral endoplasmic reticulum exit sites. *Mol Biol Cell.* 1996;7(4):631–650.
19. Loktev AV, et al. A BBSome subunit links ciliogenesis, microtubule stability, and acetylation. *Dev Cell.* 2008;15(6):854–865.
20. Wehland J, Henkart M, Klausner R, Sandoval IV. Role of microtubules in the distribution of the Golgi apparatus: effect of taxol and microinjected anti-alpha-tubulin antibodies. *Proc Natl Acad Sci U S A.* 1983;80(14):4286–4290.